Evidence Based Characterisation of Dynamic Sensitivity for Multiblock Structures -
Computational Simulation and Experimental Validation

mbsDynamics

Report on numerical simulations

8th of December 2014

Jean-François Camenen

University of Rijeka, Faculty of Civil Engineering

Contents

1 Introduction

One of the strands of the project is the computational sensitivity study on the influence of the block discretisation level and contact law in the NSCD response predictions for selected patterns of structural multi block configurations.
We present the computational study of sliding block overturning experimental study. We focused on the influence of the block discretisation and of the contact interface conditions.
Related to the dynamic characterisation of the structures, we introduce performance attributes in terms of mode of failure for a stack of three blocks.

2 Computational simulation

2.1 Non Smooth Contact Dynamic (NSCD)

Discrete numerical simulations were performed using the non-smooth contact dynamics (NSCD) method [7, 8]. This method is based on implicit time integration of the equations of motion with respect to generalized non-smooth contact laws describing non-interpenetration and dry friction between blocks. This formulation unifies the description of lasting contacts and collisions through the concept of impulse, which can be defined as the time integral of a force. The generalized non-smooth contact laws are expressed in terms of impulse $\overrightarrow{P_C}$ and formal relative velocity $\overrightarrow{\bar{V}_C}$ at contact point C. If V_{CN}^-, V_{CT}^-, V_{CN}^+ and V_{CT}^+ denote the normal and tangential relative velocities at contact point respectively before and after collision, the formal normal and tangential relative velocities are defined as follows:

$$\begin{cases} \bar{V}_{CN} &= \frac{V_{CN}^+ + e_n V_{CN}^-}{1+e_n}, \\ \bar{V}_{CT} &= \frac{V_{CT}^+ + e_t V_{CT}^-}{1+e_t}, \end{cases} \tag{1}$$

where e_n and e_t measure the inelasticity of collisions and reduce to the normal and tangential restitution coefficients in the case of binary collisions. These generalized contact laws support momentum propagation through contact networks inherent to dense assemblies of blocks. For a given time step, impulses and velocities are determined according to an iterative process using a non-linear Gauss-Seidel like method [5][2]

2.2 Contact detection algorithm

The NSCD method was applied using Solfec software which namely implements a 3D contact detection algorithm described with details in [6]. Basically, one defines mesh for each body and one computes the volumetric overlap between the two grids. Then the contact point and normal vector for each mesh of the grid is defined as respectively the barycentre of the volume and the perpendicular of the tangent plane (see figure 1). The iterative process of the solver explores each contact in order to look for a solution which satisfies the entire contact net. There is influence of block discretisation.

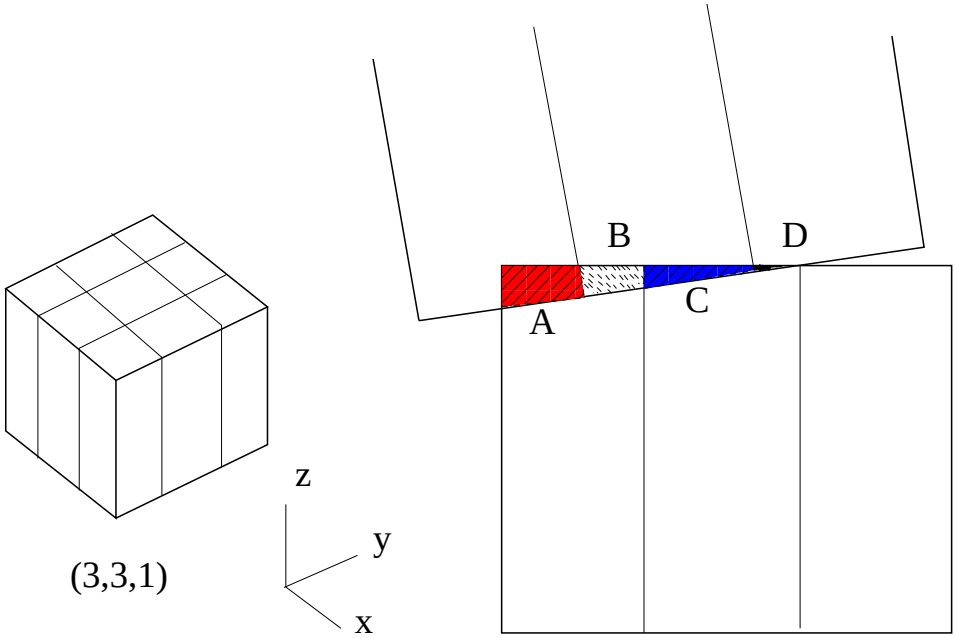

Figure 1: Mesh is defined for each body (division in 3 according to x and y) then the contact point for each mesh of the grid is defined as the barycentre of the volume, that is here A, B, C and D.

3 Computational validation of the test experiment

This preliminary experiment allows us to define physics and numerical parameters of our numerical model.

3.1 Numerical model

3.1.1 Set up

The system (see Figure 2) consists of a base ($200 * 20 * 11.8\ mm^3$) which can slide on a frame only according to one horizontal direction (Y). The frame is blocked. A block ($45 * 10 * 11.8\ mm^3$) is glued on the base.

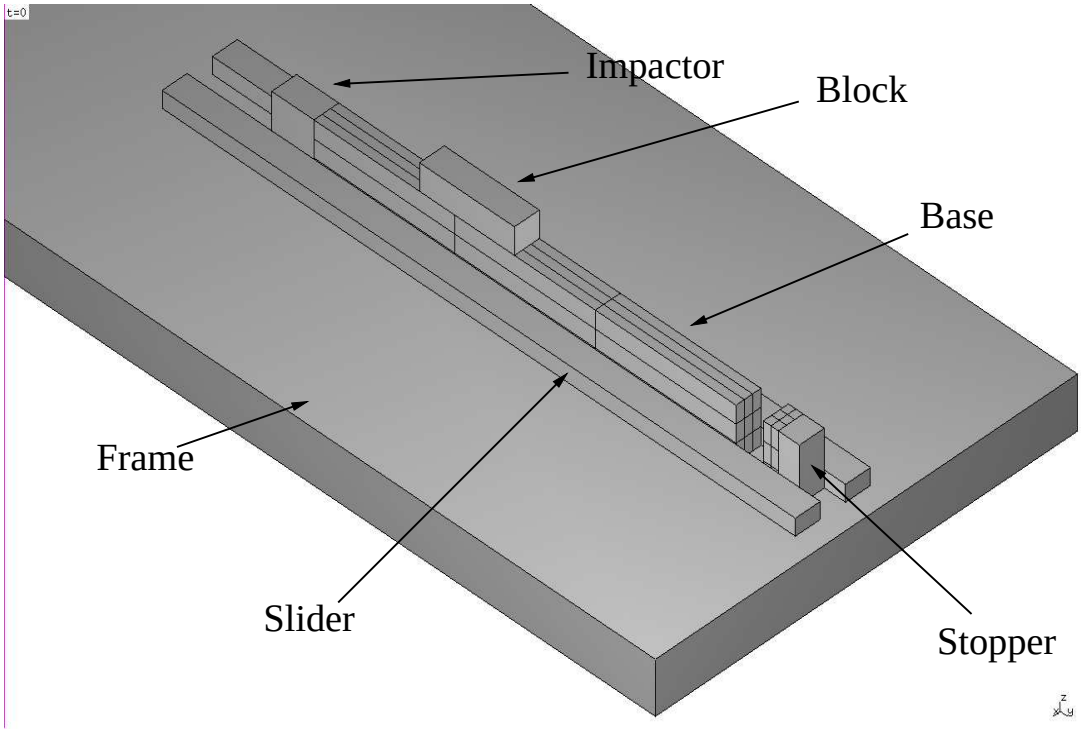

Figure 2: Numerical set up of the preliminary experiment.

An impactor in contact with the base pushes the base according to a velocity law (see Figure 3) and then goes back letting the base go freely: there is no shock, it does't model the real impactor behaviour. The base hits a deformable solid which is the piece of foam glued to the stopper, a solid body. There is a gap of 0.1 mm between sliders and the base in order to ease movement. Parameters of the impactor velocity law are $T = 0.005\ s$ and $V = 0.35\ m/s$. The initial gap G between the base and the stopper was $G = 0.02\ m$ ($0.013\ m$ with the foam). Figure 4 shows the experimental time evolution of the horizontal velocity of the system (base+block). A projectile hits the base which reaches its maximal velocity. The base moves freely until hitting the stopper ($t \approx 0.05\ s$): velocity decreases because of the friction with the frame and the sliders. The system goes back, pushed with the foam and stops.

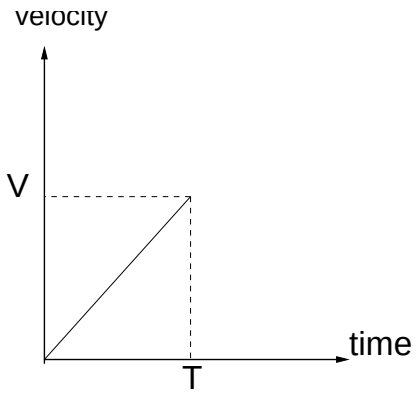

Figure 3: Velocity law applied on the base, $V = 0.35$ m/s and $T = 0.005$ s.

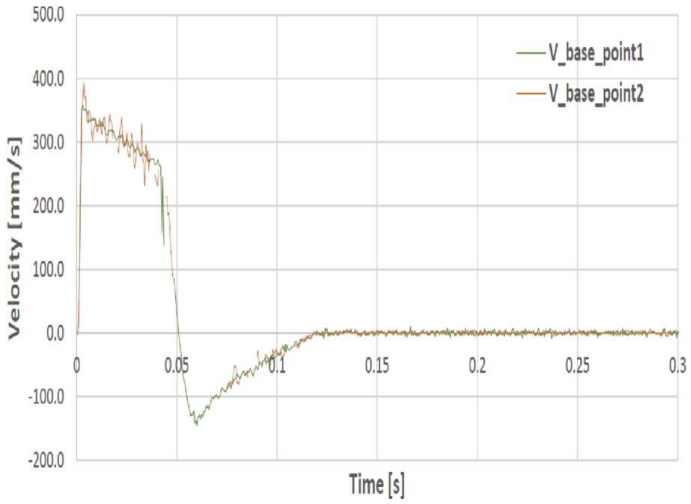

Figure 4: Experimental time evolution of the horizontal velocity of the system (base+block).

3.1.2 Physics and numerical parameters

We assume that all the bodies are rigid. Base and block are made of aluminium, the frame, the sliders and the stopper of Teflon. The physical parameters are taken as follow:

- density $\rho_{aluminium} = 2700\ kg/m^3$ and $\rho_{Teflon} = 2160\ kg/m^3$
- coefficient of restitution normal and tangential $e_n = e_t = 0$

The coefficient of friction μ between base and frame (aluminium/Teflon) is 0.2 according to [1]. But here the contact surfaces are complex, we have the frame and the sliders with geometrical imperfections. We decided to compute simulations with a coefficient friction range of 0.18 to 0.3.

The model of Kirschhoff-Saint Venant is used to describe the behaviour of the foam glued to the stopper because it uses Hook's law in combination with Green's tensor suitable for large strains. The physical parameters are taken as follow:

- Poisson coefficient: 0.18 [10]
- density foam: 40 kg/m^3

According to [10] elastic modulus E for foam is about tens of thousands Pa. We decided to compute simulations with elastic mudulus range of 40000 Pa to 140000 Pa. The model of Kirschhoff-Saint Venant has

several shortcomings, in particular the resulting hyperelastic energy is not polyconvex limiting the available existence results [3]. This can be managed by introducing a stiffness proportional damping coefficient as it is defined in Solfec code [6]. Several previous studies lead to the optimal value of 1.10^{-4} for this ratio.

For a sake of limiting time simulation we try to get the tiniest time step. The block free falling time from initial own height is the characteristic time t_C in our experiment, we find $t_C = \sqrt{\frac{15.10^{-3}}{g}} \approx 10^{-2}s$ (with $g = 9.81\ m.s^{-2}$ the gravitation constant). In order to secure our studies and in particular avoid the brake failure effect [11], we take time step $\Delta T = (1/100)t_C = 10^{-4}s$.

Block discretisation influences the result of the contact detection algorithm. One can expect that the more the blocks are discretised, the more the simulation is accurate but longer is the simulation time as well. We decided to compute simulations with different grids, defining mesh as previously: $(1, 1, 1)$, $(3, 3, 3)$, $(5, 5, 5)$, $(7, 7, 7,)$ and $(9, 9, 9)$ in order to find the optimal one.

3.2 Parametric study

3.2.1 Influence of friction μ and Young modulus E of the foam

Figures 5 and 6 show the time evolution of the horizontal velocity of the ensemble (base+block) for different values of friction coefficient between the base and the frame and for a given Young modulus of the foam. One can see pretty influence of both friction coefficient and Young modulus on the shape of the curves. The result are slightly sensitive to this parameters. By comparison with the figure 4, we get the best fit with $\mu = 0.26$ and $E = 120000$ Pa or $E = 140000$ Pa, curves don't change so much with these two values of E.

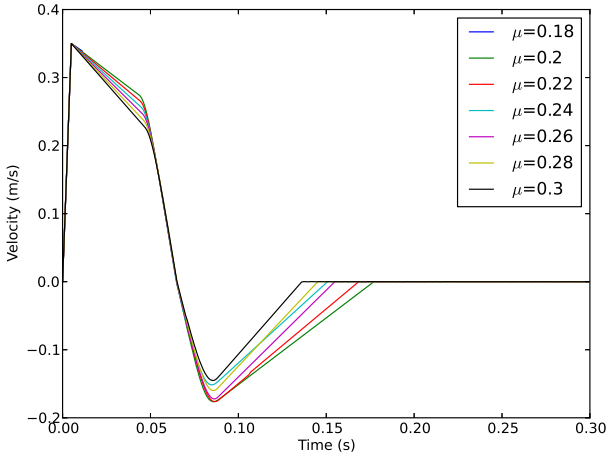

(a)

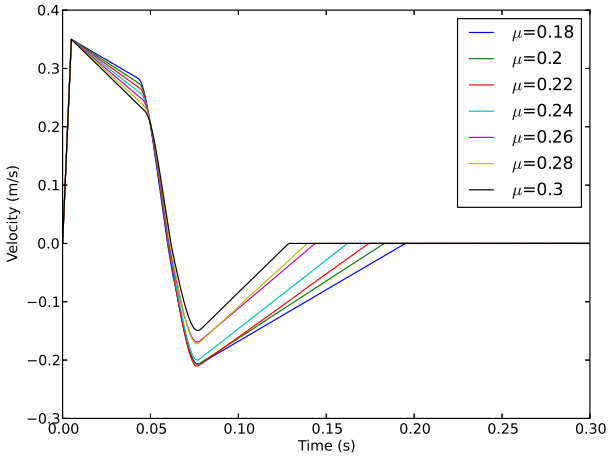

(b)

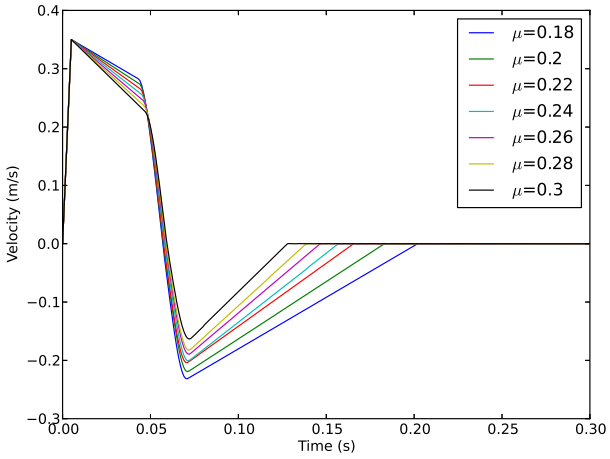

(c)

Figure 5: Time evolution of the horizontal velocity of the system (base+block) with different friction coefficient and Young modulus (*a*) $E = 40000\ Pa$ (*b*) $E = 60000\ Pa$ and (*c*) $E = 80000\ Pa$.

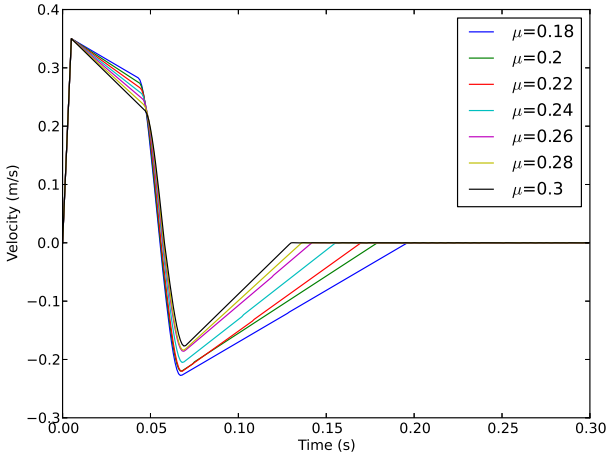

(a)

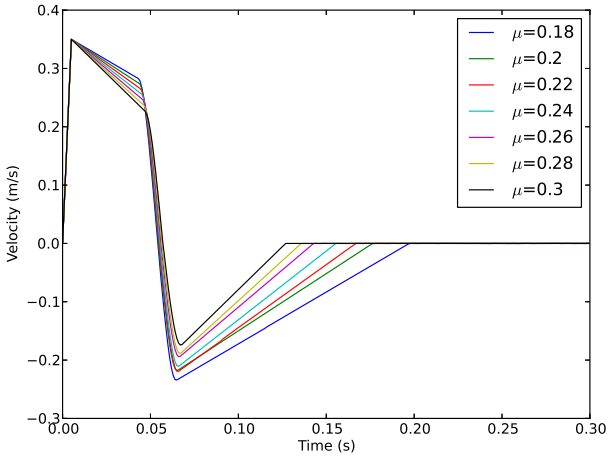

(b)

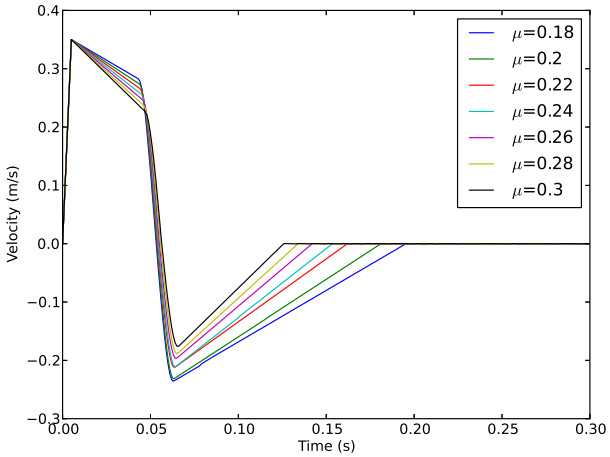

(c)

Figure 6: Time evolution of the horizontal velocity of the system (base+block) with different friction coefficient and Young modulus (*a*) $E = 100000\ Pa$ (*b*) $E = 120000\ Pa$ and (*c*) $E = 140000\ Pa$.

3.2.2 Influence of block discretisation

Figure 7 shows the time evolution of the horizontal velocity and horizontal displacement of the ensemble (base+block) for different grids for the base and parameters $\mu = 0.26$ and $E = 120000$ Pa. One can observe almost no influence of the choice of the grid.

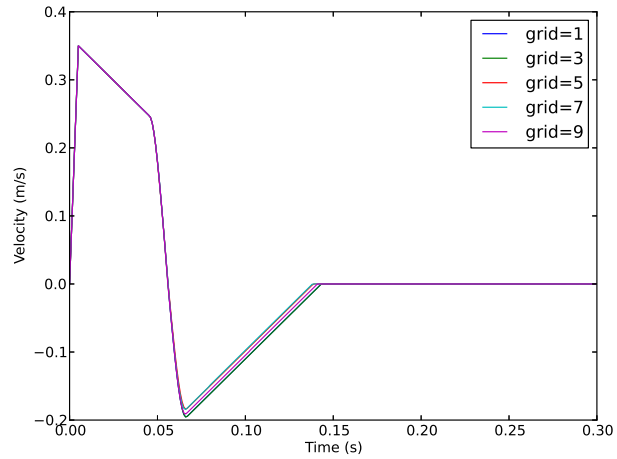

(a)

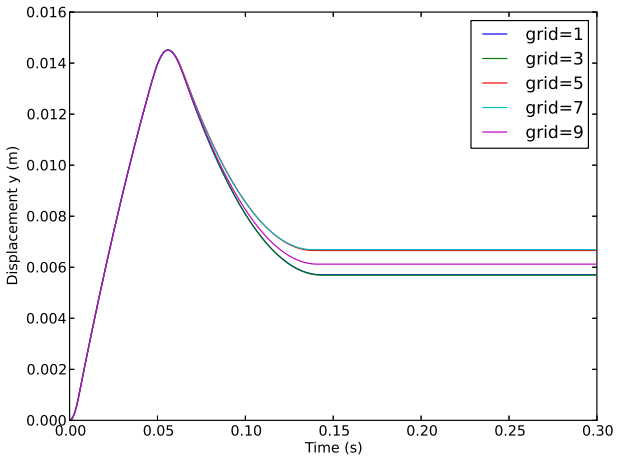

(b)

Figure 7: Time evolution with different grids of (a) the horizontal velocity and (b) the horizontal displacement of the system (base+block).

3.2.3 Discussion

We found a friction coefficient higher than the one given by [1]. This higher value allows us to take into account the actual action of the sliders on the base during the experiment because of the imperfection of the surfaces of the bodies. According to [10] elastic modulus E for foam is about tens of thousands Pa. Since there are not much differences in the results with $E = 140000$ Pa and $E = 120000$ Pa, we took the smaller one. We saw not much differences in the results with different grids as well. But the movement of the base is simple, without rocking. One can expect with free moving blocks displayed on the base more complex movement then the sensitivity to the block discretisation has to be studied.

4 Computational study of a stack of blocks

4.1 Numerical model of selected multi blocks configuration

Figure 8 shows the numerical model of the selected configuration. The system is composed of three blocks (one block: $15 * 11.8 * 10\ mm^3$) displayed on the base. The impactor pushes the base with the previous velocity law.
In this study, the range of maximal velocity V is 0.25 to 0.55 m/s and $T = 0.005\ s$. The initial gap G between the base and the stopper varies between $G = 0.024\ m$ and $G = 0.044\ m$.

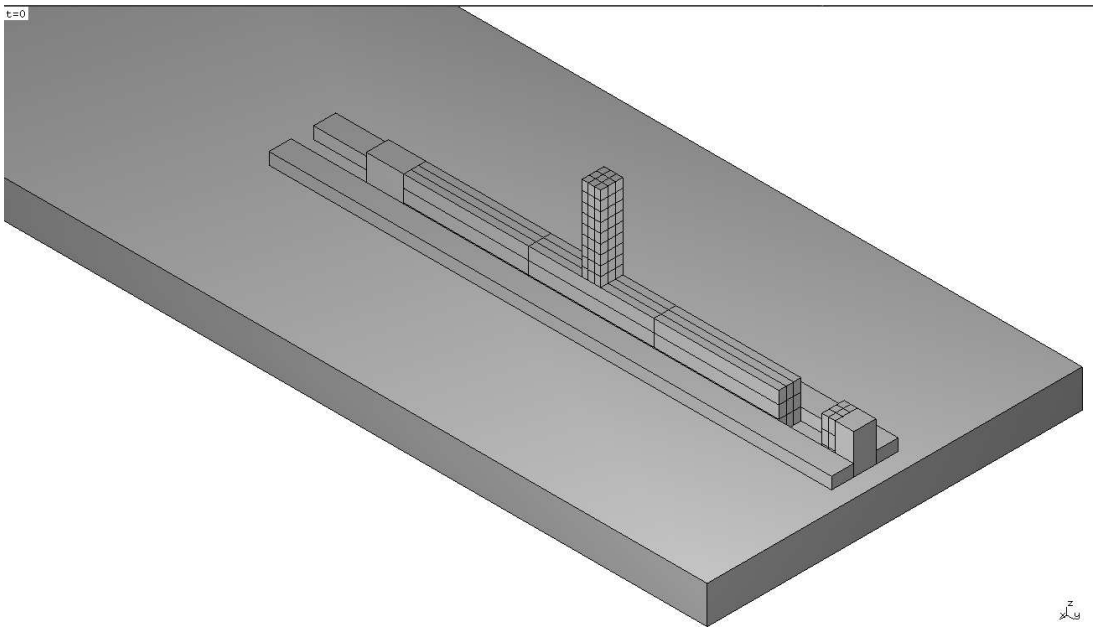

Figure 8: The system with the impactor in contact with the base, the three blocks (top, middle and bottom) displayed on it, the sliders and the stopper.

We assume that all the bodies are rigid. The other parameters are taken as follows:

- coefficient of restitution normal and tangential $e_n = e_t = 0$
- coefficient of friction (base/frame): 0.26

In the experiment, the surface of the blocks is either smooth or tough after sandblasting. The coefficient of friction (block/block) is taken 1.3 [1] when the blocks are smooth. For the blocks toughened, coefficient of friction can be twice the previous value according the study of Hisakado [4]. So we decided to compute simulations with friction coefficient between blocks in the range 1.3 to 2.7.

We apply the Kirchhoff-Saint Venant model to the foam. The physical parameters are taken as follow:

- Poisson coefficient: 0.18 [10]
- density foam: 40 kg/m^3
- Young mudulus $E = 120000$ Pa

We took the grid $(3, 3, 3)$ for the base. In order to study the sensitivity of block discretisation, we compute simulations with grids $(1, 1, 1)$ and $(3, 3, 3)$ for the blocks.

4.2 Characterisation of dynamic sensitivity

Several parameters can be suggested in order to characterise the dynamic sensitivity of structures of blocks:

- self organization
- tumbling mode
- pattern recognition
- energy loss and repartition

In this study with 3 blocks we adopted a description in terms of modes of failure. At the end of the experiment, if:

- the stack is still stable on the base → mode A
- overtuning of the top block → mode B
- overtuning of the top and middle blocks → mode C
- overtuning of the all stack → mode D

4.2.1 Influence of contact interface conditions between blocks

Time evolution of the horizontal velocity and displacement of the base (with the blocks displayed on it) with initial velocity 0.4 m/s and gap $G = 0.03$ m were computed with several values of friction coefficient in order to explore the influence of contact interface between the blocks on the entire system (see Figure 9). One can detect the influence of friction coefficient between blocks on the dynamics of the base after the impact with the stopper with the time evolution of the displacement more than the velocity: the base stopped at different distances. One can see the influence of the block discretisation on the displacement (graphs (c) and (d)): the behaviour of the blocks is different during the simulation.

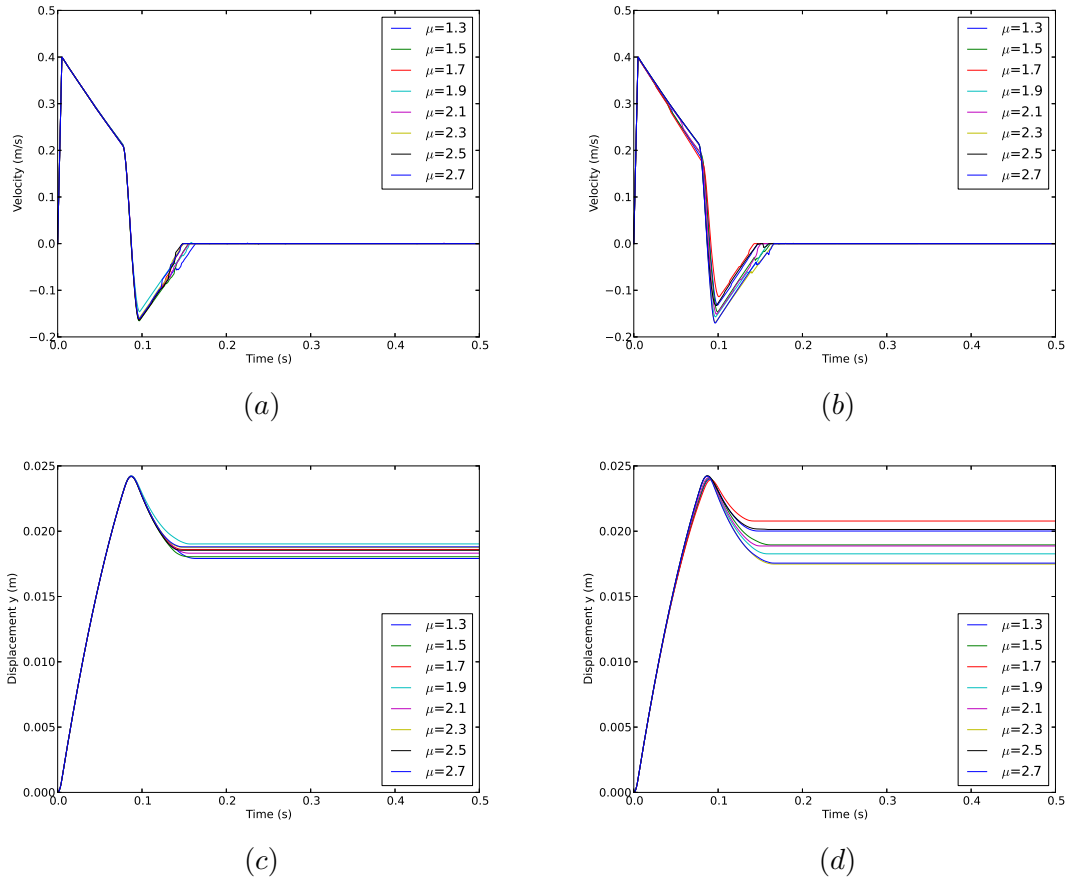

Figure 9: Time evolution of the horizontal absolute velocity according to Y of the base with (a) grid $(1, 1, 1)$ and (b) grid $(3, 3, 3)$. Time evolution of the horizontal displacement according to Y of the base with (c) grid $(1, 1, 1)$ and (d) grid $(3, 3, 3)$.

To go further, we explore Figure 10 the time evolution of the horizontal relative displacement according to Y between the top and middle blocks, the middle and bottom blocks, the bottom block and the base respectively (a), (c), (e) with grid $(1, 1, 1)$ and (b), (d), (f) with grid $(3, 3, 3)$.
The relative displacement between the blocks implies that the distribution of the mass in the system changes. The relative displacement changes with the friction then there is an influence of the contact interface on the behaviour of the structure of blocks. Nevertheless, the results are different with different grids for the blocks. In particular, with grid $(1, 1, 1)$, graph (e) shows that the bottom block stayed in the base whereas graph (f) shows that the block left the base with grid $(3, 3, 3)$. Visualisation of the simulation shows that with grid $(3, 3, 3)$ blocks had the tendency to turn around their vertical axis more than the simulations with grid $(1, 1, 1)$.

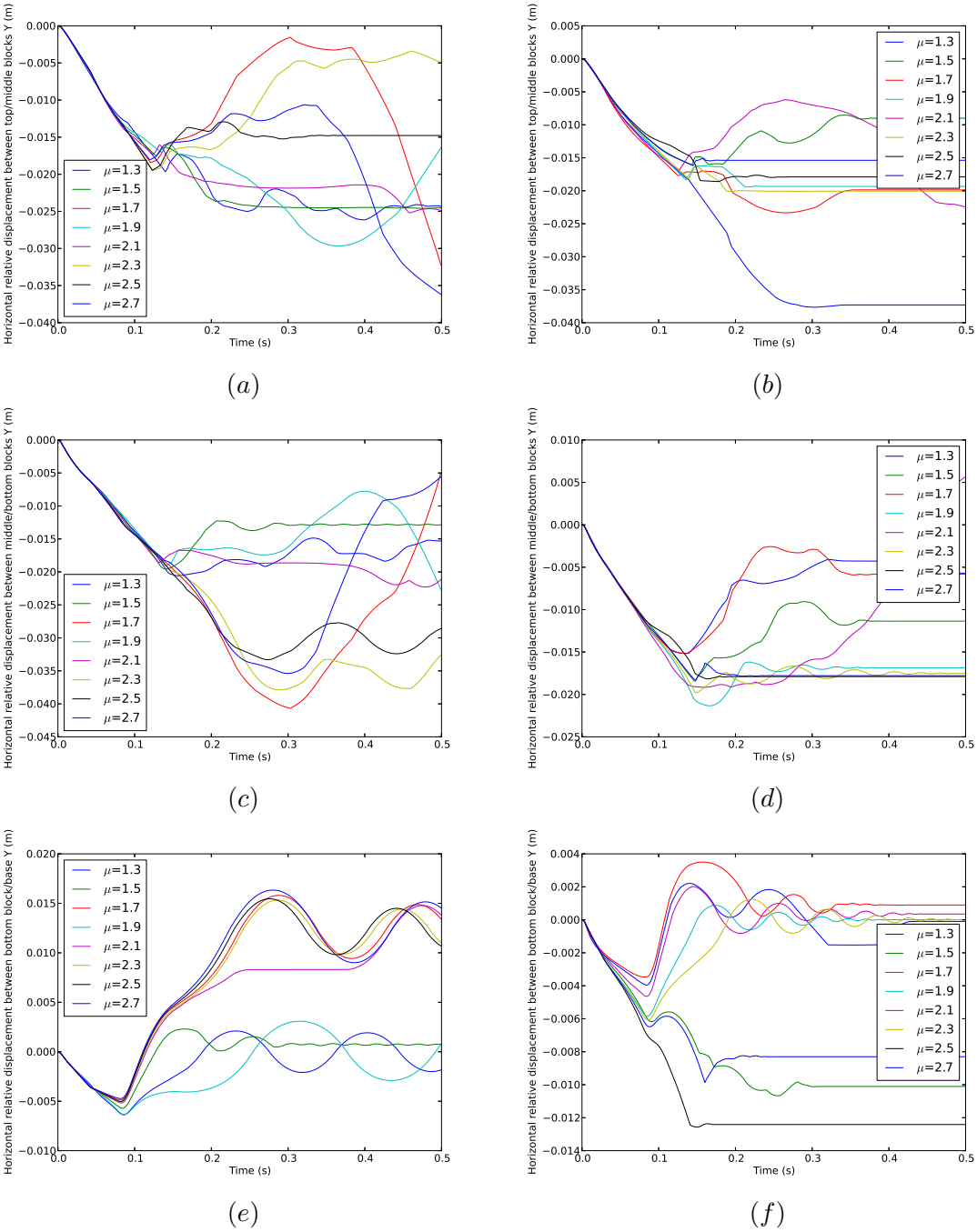

Figure 10: Time evolution of the horizontal relative displacement according to Y between the top and middle blocks, the middle and bottom blocks, the bottom block and the base respectively (a), (c), (e) with for the blocks grid $(1, 1, 1)$ and (b), (d), (f) with grid $(3, 3, 3)$.

4.2.2 Influence of energy put in the system and gap

A global analysis is presented Figure 11, Figure 12, Figure 13 and Figure 14 via modes of failure of stack of three blocks. They were lead with with the grid $(3, 3, 3)$ for the blocks.
Figure 11 shows these modes of failure related to initial velocity of the base (after being pushed by the impactor) and distance between base and stopper with different friction coefficient between the blocks. The system reach the stopper all the time then it experiences different modes with the distance (G) between base and stopper. Friction coefficient between blocks influences the results, the graphs are not exactly the same which shows the influence of contact interface properties. The modes A and B never appear.

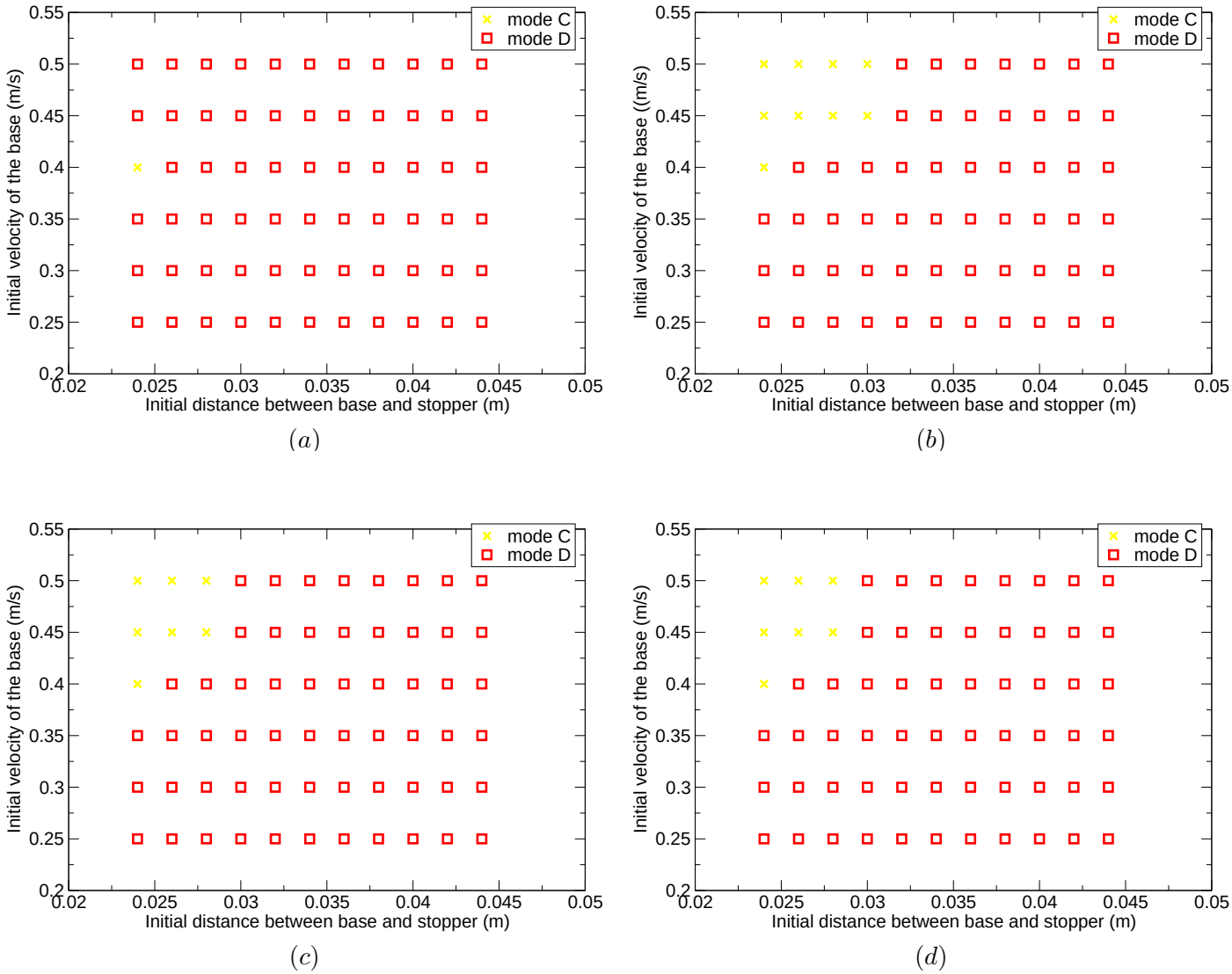

Figure 11: Modes of failure of stack of three blocks related to initial velocity of the base and distance (G) between base and stopper with different friction coefficient between the blocks (a) 1.3, (b) 1.7, (c) 2.1 and (d) 2.5.

Figure 12 shows modes of failure of stack of three blocks related to initial velocity of the base and distance between base and stopper emphasizing on the region where the modes change.

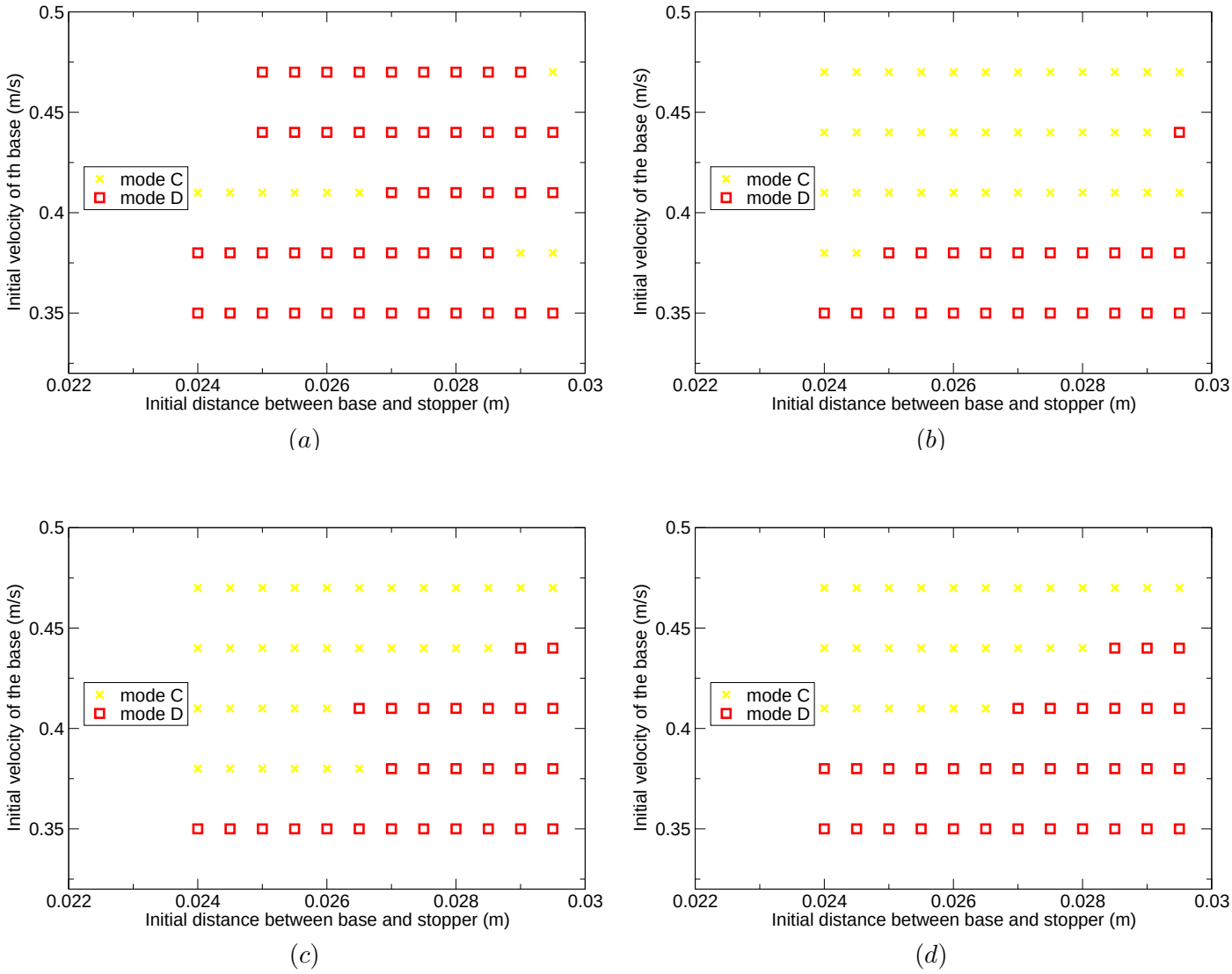

Figure 12: Modes of failure of stack of three blocks related to initial velocity of the base and distance (G) between base and stopper with different friction coefficient between the blocks (a) 1.3, (b) 1.7, (c) 2.1 and (d) 2.5.

Figure 13 shows modes of failure of stack of three blocks related to initial kinetic energy of the ensemble (base+blocks) and free moving time of the base with different friction coefficient between the blocks. Graphs are pretty different showing the influence of contact interface properties.

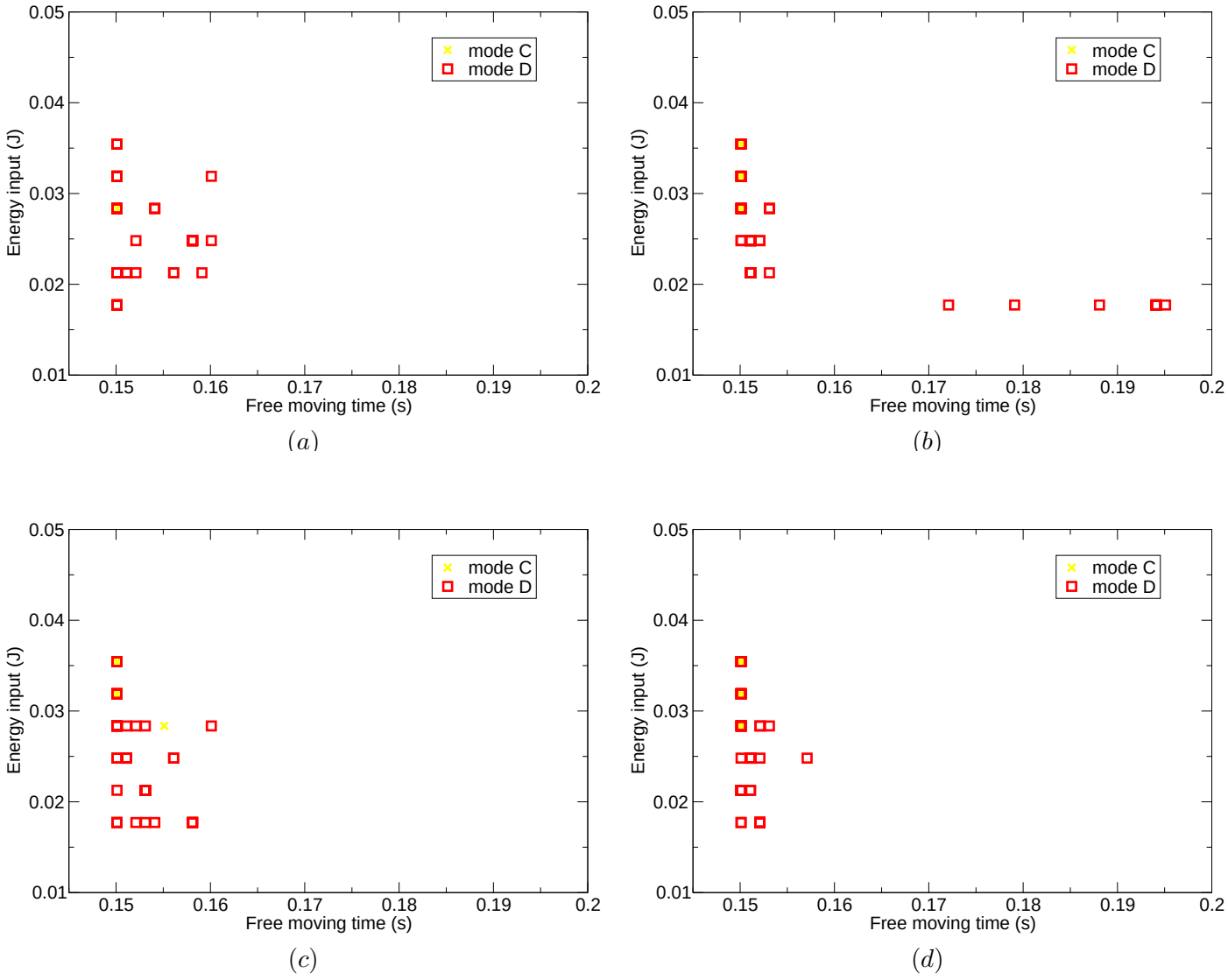

Figure 13: Modes of failure of stack of three blocks related to initial kinetic energy of the ensemble (base+blocks) and free moving time of the base with different friction coefficient between the blocks (*a*) 1.3, (*b*) 1.7, (*c*) 2.1 and (*d*) 2.5.

Figure 14 shows modes of failure of stack of three blocks related to initial kinetic energy of the ensemble (base+blocks) and free moving time of the base emphasizing on the region where the modes change.

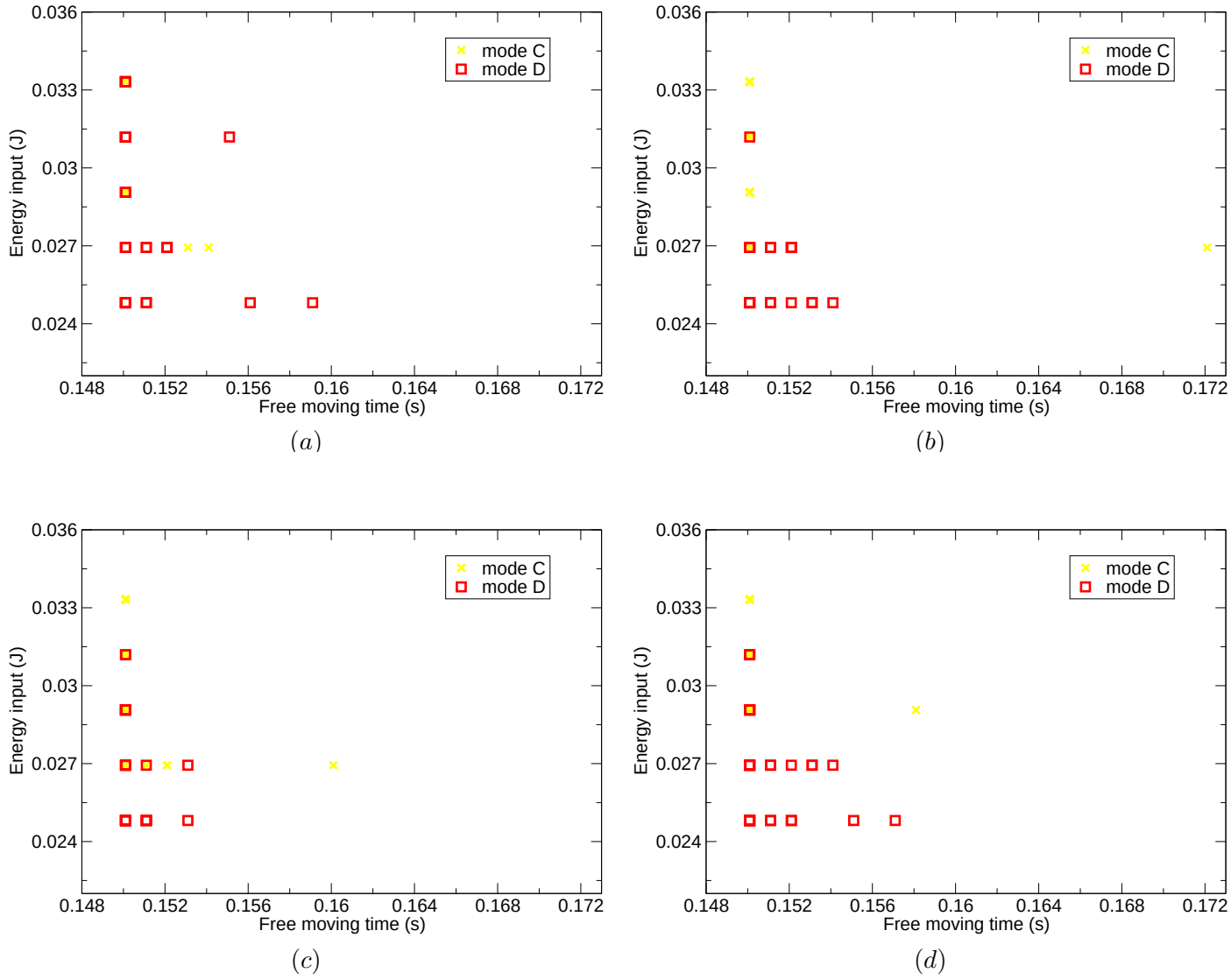

Figure 14: Modes of failure of stack of three blocks related to initial kinetic energy of the ensemble (base+blocks) and free moving time of the base with different friction coefficient between the blocks (*a*) 1.3, (*b*) 1.7, (*c*) 2.1 and (*d*) 2.5.

5 Conclusions & perspectives

The computational validation of single non sliding and the computational study of sliding block overturning experimental study showed the influence of the block discretisation and the influence of the contact interface conditions.
In the study with a stack of 3 blocks the dynamic characterisation consisted in the definition of 4 modes of failure. This approach allowed us to show the influence of the contact interface between the blocks.
For the future study with structures of stacks, this definition in terms of modes of failure is less suitable. Inspired by physics of condensed matter, one can use the radial distribution function [9] (or pair correlation function) for the centres of mass of the particles to examine translational order in a granular material.

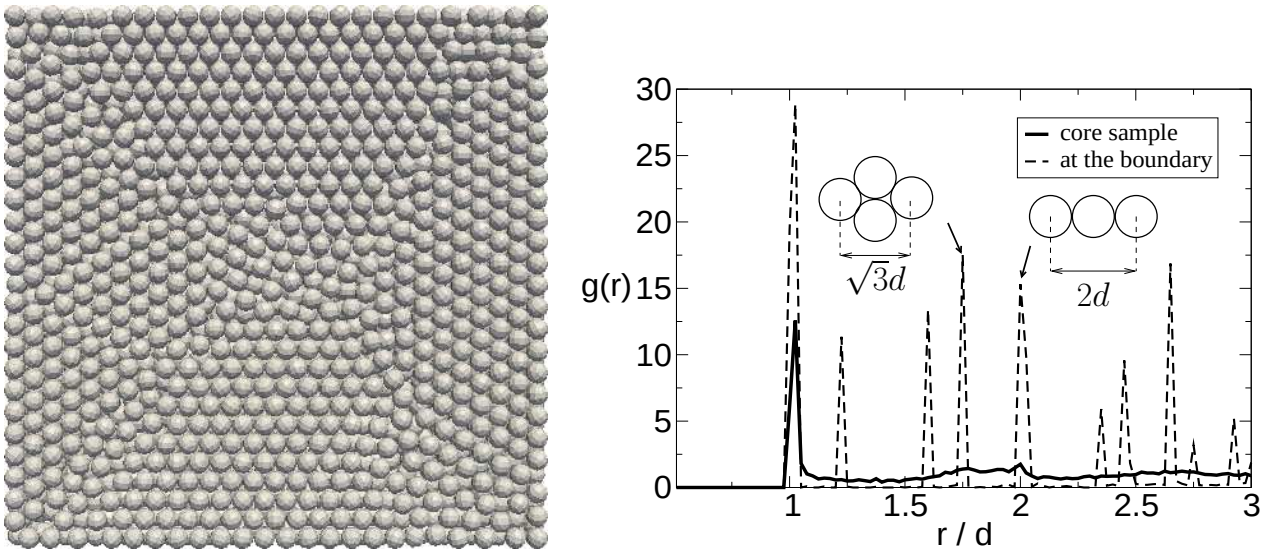

(a) (b)

Figure 15: (a) bottom view (wall removed) of a packing of spheres (built by pluviation). In contact with the wall particles are strongly arranged. (b) pair correlation function computed at the core of the packing and just near the walls.

References

[1] P. J. Blau. *Friction Science and Technology: From Concepts to Applications*. 2009.

[2] F. Dubois and M. Jean. Lmgc90 : Une Plateforme de Développement Dédiée à la Modélisation des Problèmes d'Interaction. *Actes du sixième colloque national en calcul des structures CSMA-AFM-LMS*, 1:111–118, 2003.

[3] M. Hauth. *Visual Simulation of Deformable Models*. PhD thesis, Fakultat fur Informations and Kognitionswissenschaftens der Eberhard-Karls Universitat Tubingen, 2004.

[4] T. Hisakado. On the mechanism of contact between solid surfaces (4 th report, surface roughness effects on dry friction). *Bulletin of the Japan Society of Mechanical Engineers*, 13:129–139, 1970.

[5] M. Jean. The non-smooth contact dynamics method. *Computer Methods in Applied Mechanics Engineering*, 177:235–257, 1999.

[6] T. Koziara and N. Bećanić. A distributed memory parallel multibody contact dynamics code. *Int. Journal for Numerical Methods in Engineering*, 87:437–456, 2011.

[7] J.J. Moreau. Some Numerical Methods in Multibody Dynamics : Application to Granular Materials. *European J. Mech. A*, 13:93–114, 1994.

[8] J.J. Moreau and M. Jean. Numerical treatment of contact and friction : the contact dynamics method. *Engineering systems design and analysis*, pages 201–208, mars 1996.

[9] L.E. Silbert, D. Ertas, G.S. Grest, T.C. Halsey, and D. Levine. Geometry in Frictionless and Friction Sphere Packings. *Phys. Rev. E*, 65:031304, 2002.

[10] Benjamin Sobac, Mathieu Colombani, and Yoel Forterre. Dynamique de Mousses Poroélastiques. *Mécanique & Industries*, 12:231238, 2011.

[11] T. Unger, L. Brendel, D.E. Wolf, and J. Kertèsz. Elastic behavior in contact dynamics of rigid particles. *Phys. Rev. E*, 65:061305, 2002.